

Poly(di-*n*-propylsilylene) and Poly(diethylsilylene-co-di-*n*-propylsilylene): Solid State Structure and Phase Transitions

Rogério Menescal, Jeffrey Eveland, and Robert West*

Chemistry Department, University of Wisconsin—Madison, Madison, Wisconsin 53706-1396

Larissa L. Leites, Sergey S. Bukalov, and Tatiana D. Yadritseva

Institute of Organo-element Compounds, Scientific and Technical Center on Raman Spectroscopy, Russian Academy of Sciences, 117312 Moscow, Russia

Marianne Blazsó

Research Laboratory for Inorganic Chemistry, Hungarian Academy of Sciences, H-1112 Budapest, Hungary

Received November 24, 1993; Revised Manuscript Received June 7, 1994*

ABSTRACT: Poly(di-*n*-propylsilylene) and poly(diethylsilylene-co-di-*n*-propylsilylene) have been investigated by Raman, IR, and UV spectroscopy, TGA, DSC, wide angle X-ray diffraction, and solid state ^{13}C and ^{29}Si NMR. No IR-Raman coincidences were found in the Si—Si or Si—C stretching regions for $(n\text{-Pr}_2\text{Si})_n$, demonstrating that the main chain has a planar *all-trans* configuration, T_∞ , consistent with the UV absorption at 355 nm. From the Si—C stretching bands, all of the *n*-propyl groups appear to have the same conformation. $(n\text{-Pr}_2\text{Si})_n(\text{Et}_2\text{Si})_m$ also has the T_∞ configuration at room temperature, and a tetragonal crystal lattice. Both polymers undergo a first-order transition to a mesomorphic phase, above 222 °C for $(n\text{-Pr}_2\text{Si})_n$ and above 113 °C for the copolymer.

I. Introduction

The polysilane high molecular weight polymers, or poly(silylene)s, have attracted considerable attention, partly because of their unusual electronic and photophysical properties associated with the delocalization of σ -electrons along the polysilane chain.¹ In addition these polymers have numerous potential technological applications.

The structures of the di-*n*-alkylpolysilanes have been investigated using a variety of techniques. Poly(dimethylsilylene) $[(\text{Me}_2\text{Si})_n]$,^{2,3} poly(diethylsilylene) $[(\text{Et}_2\text{Si})_n]$,³⁻⁵ and poly(di-*n*-propylsilylene) $[(n\text{-Pr}_2\text{Si})_n]$ ⁴ all have been shown to have a planar, *all-trans* zigzag (T_∞) structure for the main polymer chain. Poly(di-*n*-butylsilylene)^{6,7} and poly(di-*n*-pentylsilylene)^{7,8} however, adopt 7/3 helical structures under ambient conditions. The *all-trans* structure returns with six-carbon side chains; the well-studied poly(di-*n*-hexylsilylene) has the T_∞ structure up to its transition temperature at 42 °C and a mesomorphic structure above that.⁹⁻¹¹ Poly(di-*n*-heptylsilylene) also takes the T_∞ structure at ambient temperatures.^{10,12}

Here we report a study of $(n\text{-Pr}_2\text{Si})_n$ and the related polysilane copolymer poly(diethylsilylene-co-di-*n*-propylsilylene), $(n\text{-Pr}_2\text{Si})_n(\text{Et}_2\text{Si})_m$. Our results confirm the T_∞ conformation for poly(di-*n*-propylsilylene), reported from earlier electron and X-ray diffraction studies,⁴ and show that at room temperature the copolymer also has a planar zigzag conformation of the silicon chain. These results also allow a closer description of the structures, especially at elevated temperatures where both polymers have a first-order phase transition.

II. Results and Discussion

A. Poly(di-*n*-propylsilylene) at Room Temperature. The ultraviolet spectrum of $(n\text{-Pr}_2\text{Si})_n$ was previously reported to consist of three peaks at 312, 324, and 360 nm, but the earlier authors considered that impurities

might be present in their sample.^{4a} The UV spectrum of $(n\text{-Pr}_2\text{Si})_n$, purified as described in the Experimental Section, showed only a single absorption band at 355 nm (Figure 1), similar to that reported for $(\text{Et}_2\text{Si})_n$ at 352 nm.^{4a}

The Raman spectrum of polycrystalline $(n\text{-Pr}_2\text{Si})_n$ was determined from 5 to 3400 cm^{-1} , and the infrared spectrum from 150 to 3400 cm^{-1} ; the results are presented in Figure 2 and Table 1. At room temperature the polymer spectral bands are rather narrow, indicating no significant disorder in the crystal.¹³ Band assignments were made by analogy with the detailed spectral studies of oligomeric Si_3Me_8 ¹⁴ and $\text{Si}_4\text{Me}_{10}$ ¹⁵ and polymeric $(\text{Me}_2\text{Si})_n$,^{3b} and $(\text{Et}_2\text{Si})_n$,⁵ and also by comparison with the spectrum of the model compound Pr_2SiCl_2 . For the latter, depolarization ratios of the Raman lines were measured.

The vibrational spectrum of $(n\text{-Pr}_2\text{Si})_n$ with its structural unit $(\text{SiPr}_2\text{—SiPr}_2)$ should exhibit two Si—Si stretching vibrations in the region 300–500 cm^{-1} and four Si—C stretching vibrations in the region 600–750 cm^{-1} . As is evident from the spectra obtained (Figure 2), the rule of mutual exclusion applies to the skeletal vibrations. The two Raman lines of $\nu_{\text{Si—Si}}$, at 446 and 472 cm^{-1} , have no counterparts in the IR spectrum. Of the four $\nu_{\text{Si—C}}$ vibrations, two are seen in the Raman and two in the IR spectrum. Such strict selection rules are consistent with the D_{2h} symmetry of the repeat structural unit (the distribution of the polymer skeletal vibrations among symmetry species in terms of the D_{2h} symmetry group was given in ref 3b). As in the cases of $(\text{Me}_2\text{Si})_n$ ^{3b} and $(\text{Et}_2\text{Si})_n$,⁵ these facts lead to the unambiguous conclusion that the main chain of $(n\text{-Pr}_2\text{Si})_n$ also has a planar *trans* conformation T_∞ . The same conclusion was reached by Lovinger *et al.* from electron diffraction measurements.^{4a}

The simple pattern observed from 600 to 750 cm^{-1} for $(n\text{-Pr}_2\text{Si})_n$ suggests that *n*-Pr tails are all in the same conformation. To see how nonrigidity in the *n*-Pr group might manifest itself in the Raman spectrum, we studied as a model compound $n\text{-Pr}_2\text{SiCl}_2$, which exhibits no steric

* Abstract published in *Advance ACS Abstracts*, August 15, 1994.

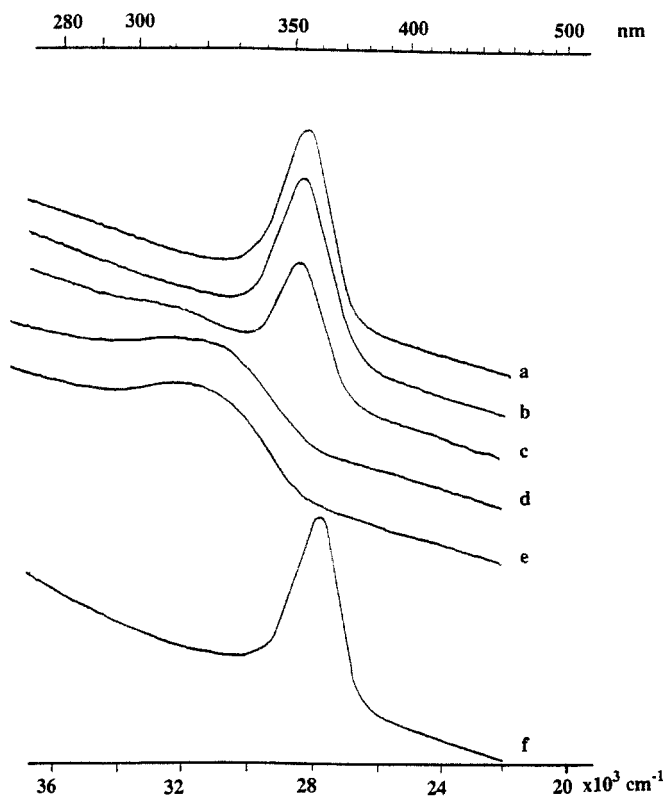


Figure 1. Temperature evolution of the UV spectrum of solid $(n\text{-Pr}_2\text{Si})_n$ at (a) 20 °C, (b) 180 °C, (c) 230 °C, (d) 250 °C, and (e) 280 °C and (f) cooled back to 25 °C.

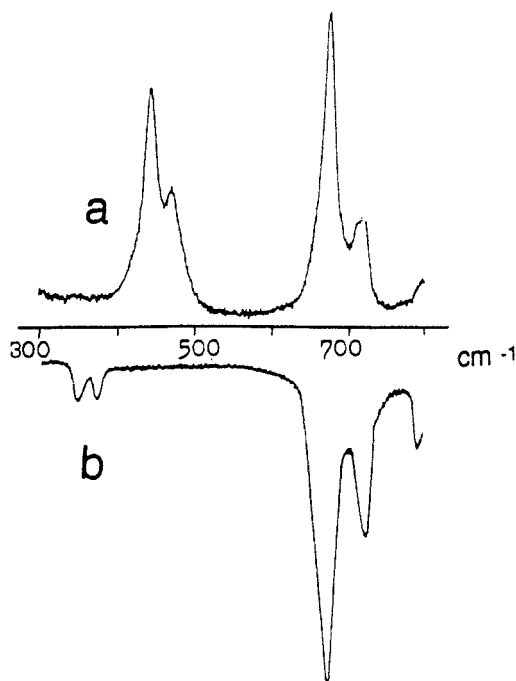


Figure 2. Raman (a) and IR (b) spectra of crystalline $(n\text{-Pr}_2\text{Si})_n$ in the region of Si-Si and Si-C vibrations.

hindrance to internal rotation. The results are presented in Figure 3, where the spectrum of the liquid at room temperature is compared to that in the solid state at -170 °C. At room temperature a complicated pattern in the $\nu_{\text{Si-C}}$ region is observed along with a doubling of a band near 900 cm^{-1} , which might include the $\nu_{\text{C-C}}$ stretch. These facts are indicative of the presence of different conformers. On cooling to -170 °C, some bands disappear. Only one line at 898 cm^{-1} remains in the $\nu_{\text{C-C}}$ region and the pattern in the $\nu_{\text{Si-C}}$ region becomes less complex, but the latter

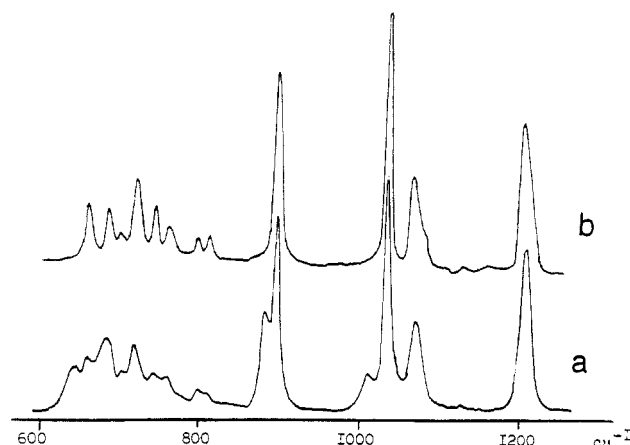


Figure 3. Manifestation of rotational isomerism in the Raman spectrum of a model compound $(n\text{-Pr}_2\text{SiCl}_2)$: (a) liquid at 25 °C; (b) solid sample at -170 °C.

Table 1. IR and Raman Spectra of a Solid Sample of $(n\text{-Pr}_2\text{Si})_n$

Raman	IR	assgnt
94 (w)		
131 (w)		
202 (s)		
252 (w)		
281 (w)	280 (vw)	
	350 (w)	
	375 (w)	
445 (s)		$\nu_{\text{Si-Si}}$
470 (m)		$\nu_{\text{Si-Si}}$
	670 (s)	$\nu_{\text{Si-C}}$
676 (vs)		$\nu_{\text{Si-C}}$
719 (m)	720 (m)	$\nu_{\text{Si-C}}$
	745 (vw sh)	
796 (w)	795 (w)	
806 (w sh)		
	835 (vw sh)	
896 (m)	900 (w)	
931 (w sh)		
991 (vw)	990 (m sh)	
1001 (vw)	998 (m)	
1025 (m)	1032 (w)	
1061 (w sh)		
1070 (w)	1068 (m sh)	
	1078 (m)	
1200 (s)	1200 (w sh)	
	1215 (w)	
	1250 (vw)	
1289 (w)		
1321 (w)		
	1329 (m)	
1376 (vw)	1380 (m)	
1416 (w)	1420 (m)	
1452 (m)	1455 (m sh)	
	1465 (m)	

still contains many more bands than theory predicts for a single conformer and than are observed in the spectrum of the polymer $(n\text{-Pr}_2\text{Si})_n$. Probably, $n\text{-Pr}_2\text{SiCl}_2$ does not crystallize and at -170 °C forms a metastable glass, in which several conformers are still present.

Thus, the model compound $n\text{-Pr}_2\text{SiCl}_2$ does exhibit rotational isomerism about the Si-C and C-C bonds, which manifests itself as a complex Raman spectrum in the corresponding regions. The absence of such complications in the Raman spectrum of $(n\text{-Pr}_2\text{Si})_n$ confirms that the n -propyl groups in the polymer exist in a single conformation.

The X-ray pattern at room temperature (Figure 4b) is very similar to the one obtained by Lovinger *et al.*,^{4a} except that the reflection at 3.70 Å indexed as 101 in a one-chain square lattice ($a = b = 0.980$ nm) is much sharper,

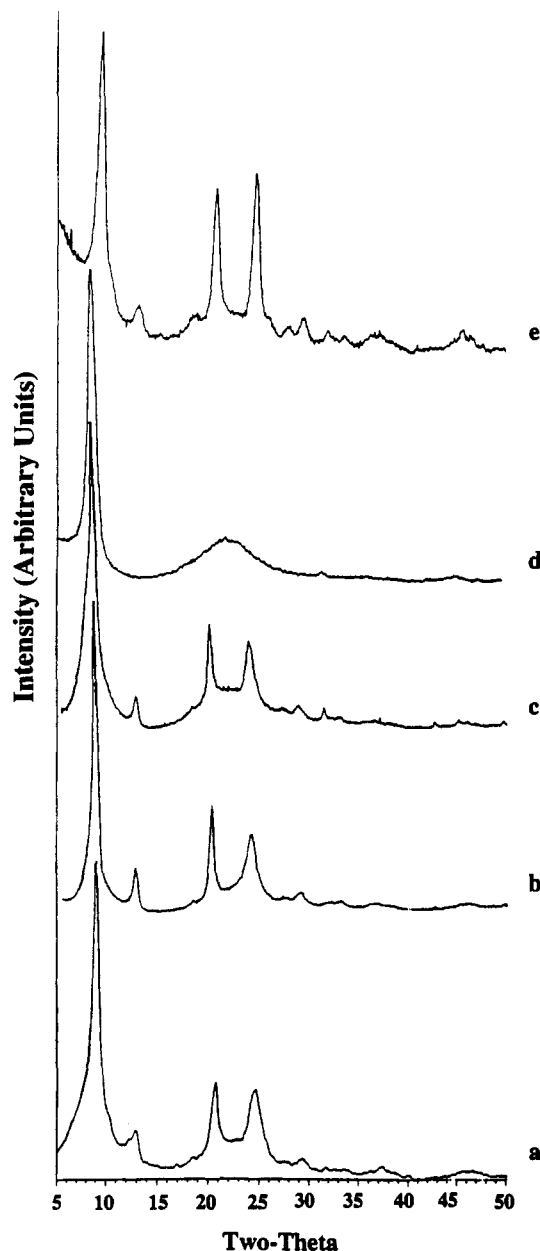


Figure 4. WAXD of $(n\text{-Pr}_2\text{Si})_n$ at (a) -40°C , (b) 25°C , (c) 160°C , and (d) 240°C , and (e) back to 25°C .

indicating more regularity in the direction of the axis that contains the polymer backbone. This is confirmed by the narrowness of the Raman lines at room temperature, indicating no significant disorder (Figure 2). Thus, all the methods used allowed us to conclude that at room temperature the polymer $(n\text{-Pr}_2\text{Si})_n$ is highly crystalline and well-ordered with T_∞ conformation of the main silicon chain and all the *n*-Pr tails in one and the same conformation.

Variable-Temperature Studies of $(n\text{-Pr}_2\text{Si})_n$. Poly(di-*n*-propylsilylene) was reported to undergo a phase transition when heated to 134°C ;^{4a} however in none of our experiments do we find evidence for a phase transition at that temperature. The DSC of $(n\text{-Pr}_2\text{Si})_n$ in Figure 5 showed two clear transitions, a weak one at -17.0°C (onset at -29°C) with $\Delta H = 0.66\text{ kJ/mol}$ and a sharp intense peak at 235°C (onset at 222°C), which corresponds to a first-order transition with $\Delta H = 7.3\text{ kJ/mol}$ (0.064 kJ/g , 15.2 cal/g). Low-temperature transitions similar to that at -29°C have also been observed for $(\text{Me}_2\text{Si})_n$ at -34°C ($\Delta H = 0.16\text{ kJ/mol}$)¹⁶ and $(n\text{-Pen}_2\text{Si})_n$ at -20°C ($\Delta H = 1.1\text{ kJ/mol}$).¹⁶

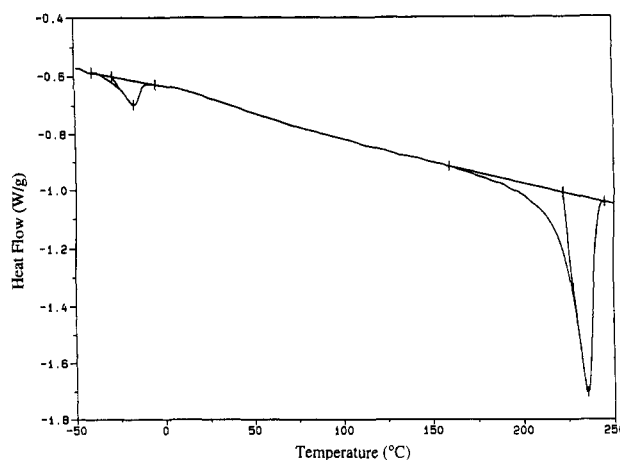


Figure 5. DSC of $(n\text{-Pr}_2\text{Si})_n$ obtained at a heating rate of 10°C/min , after cooling the sample from $+240$ to -60°C at 10°C/min .

In order to understand the structural changes associated with the DSC transitions the $(n\text{-Pr}_2\text{Si})_n$ sample was studied by variable-temperature X-ray diffraction, Raman, and UV spectroscopy.

X-ray diffractograms of $(n\text{-Pr}_2\text{Si})_n$ taken at different temperatures are shown in Figure 4. On heating to 160°C (Figure 4c), an amorphous halo centered at $2\theta = 22^\circ$ became evident but the overall pattern of peaks was preserved with only a slight decrease in intensity of lines and expansion of the lattice. The fact that no significant broadening of the 101 reflection at 3.79 \AA was detected suggests that no major structural changes along the backbone axis take place up to 160°C . Above the first-order DSC transition near 222°C (Figure 4d), all the lines disappeared except for the main peak at $2\theta = 10^\circ$ and an amorphous halo centered at $2\theta = 22^\circ$. This pattern indicates that orientational order of the polymer chains is maintained, although the *all-trans* conformation of the silicon backbone and the ordered arrangement of the side chains is disrupted. Phase transitions from crystalline to a columnar hexagonal mesophase have been reported for $(n\text{-Hex}_2\text{Si})_n$, $(n\text{-Pen}_2\text{Si})_n$, and $(n\text{-Bu}_2\text{Si})_n$, in which the silicon backbones become conformationally disordered but pack laterally in a two-dimensional hexagonal lattice.^{12,17} In the case of $(n\text{-Pr}_2\text{Si})_n$, however, the absence of higher order reflections from the peak at $2\theta = 10^\circ$ is more consistent with a nematic mesophase. Although the changes in the X-ray pattern were reversible upon cooling from 240°C (Figure 4e), the thermogravimetric analysis of $(n\text{-Pr}_2\text{Si})_n$ (Figure 6) shows that slight decomposition occurs as the polymer is heated through the first-order DSC transition at 222°C . At 250°C weight loss was 3% and decomposition ensued rapidly above 338°C . Examination of $(n\text{-Pr}_2\text{Si})_n$ by cross-polarized microscopy showed that the sample maintained birefringence up to a temperature of 350°C , after which it became isotropic due to extensive decomposition.

The Raman spectrum of $(n\text{-Pr}_2\text{Si})_n$ as a function of temperature is shown in Figure 7. On heating the sample to ca. 100°C no significant changes in the spectral pattern were revealed, indicating no changes in the molecular and crystal structure. On further heating to about 195°C , band broadening was observed (Figure 7c), along with an overall decrease in intensity, typical for all the crystalline poly(di-*n*-alkylsilylene)s studied on approaching their first-order phase transitions above room temperature.¹⁸ These changes indicate that the crystal structure is less perfect¹³ and that some reorientational molecular motions may be taking place. The latter view is confirmed by a gradual

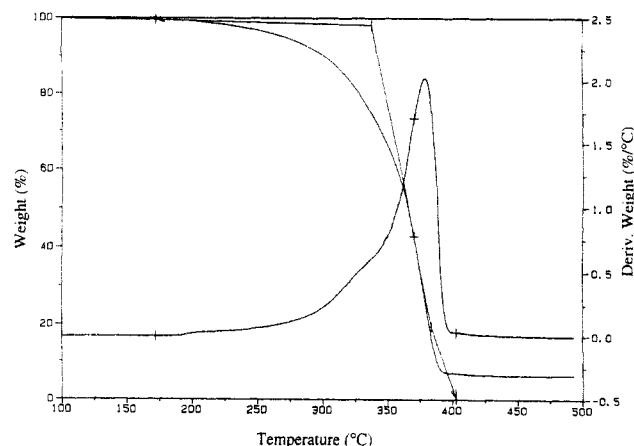


Figure 6. Thermogravimetric analysis of $(n\text{-Pr}_2\text{Si})_n$ under N_2 flow at a heating rate of $10^\circ\text{C}/\text{min}$.

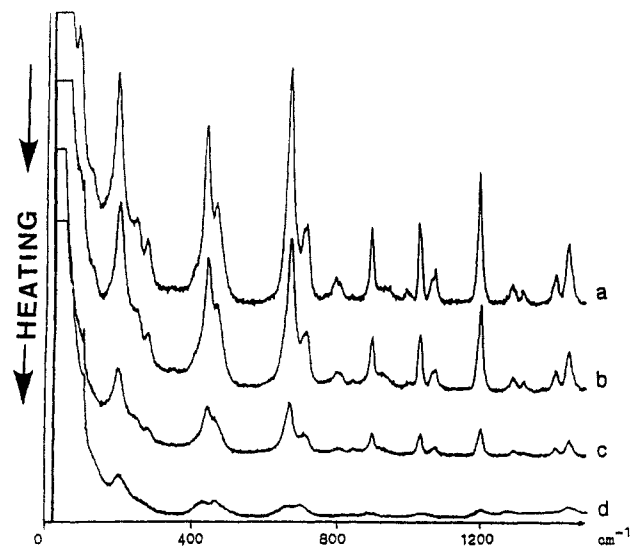


Figure 7. Temperature evolution of the Raman spectrum of $(n\text{-Pr}_2\text{Si})_n$ at (a) 25°C , (b) 100°C , (c) 195°C , and (d) 225°C .

increase with temperature in the intensity of the Rayleigh wing in the low-frequency region.¹⁹ However, no new lines appeared either in the $\nu_{\text{Si-Si}}$ or in the $\nu_{\text{Si-C}}$ and $\nu_{\text{C-C}}$ regions, which means that the average conformations of silicon backbone and propyl side chains are preserved. The absence of rotational isomerism in the $n\text{-PrSi}$ fragments of the polymer on raising the temperature is in contrast with the results for $(\text{Et}_2\text{Si})_n$,⁵ which displays rotational isomerism about the Si-C bonds in the Si-Et fragments even at 50°C . However, examination of molecular models of these polymers show that the difference is quite understandable. Unlike the ethyl groups, the more voluminous propyl substituents have no room for internal rotation in the crystal lattice of the planar *trans* polymer.

Further heating to 225°C led to a sharp drop in intensity of the original Raman lines (Figure 7d), analogous to that observed for $(n\text{-Hex}_2\text{Si})_n$ above its phase transition to a mesomorphic state at 50°C .^{9,11} The Raman spectrum of the $(n\text{-Pr}_2\text{Si})_n$ disordered phase, not being enhanced by resonance, could then be observed only using more severe registration conditions. The change in the spectrum was reversible, and there was no indication in the IR spectrum of polymer degradation during the heating process.

The variable-temperature UV measurements (Figure 1) of $(n\text{-Pr}_2\text{Si})_n$ were carried out in a high-vacuum cell. The low-temperature (20°C) absorption at 355 nm associated with an *all-trans* conformation of the silicon

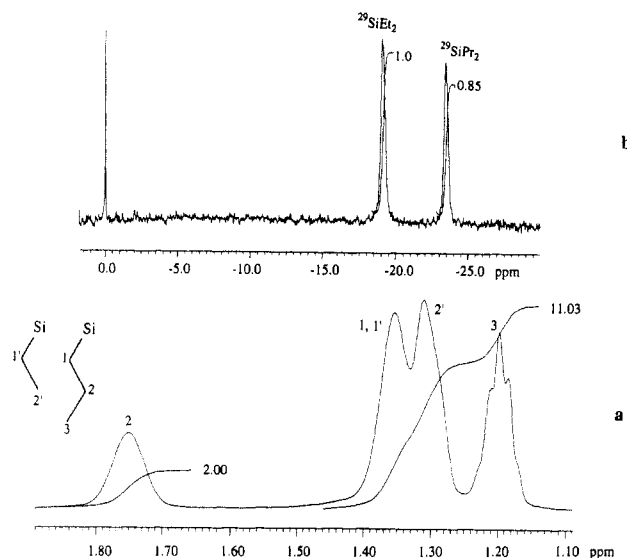


Figure 8. Integrated NMR spectrum of $(n\text{-Pr}_2\text{Si})_n(\text{Et}_2\text{Si})_m$ in benzene- d_6 : (a) ^1H (500 MHz) and (b) ^{29}Si (100.33 MHz).

backbone remains basically unchanged up to 220°C . Between about 220 and 250°C , the band gradually disappears and a new, broader band grows in at about 315 nm . This thermochromic change is fully reversible. The shift to a shorter wavelength is consistent with disruption of the *all-trans* conformation above the transition temperature. Thus, the phase transition near 230°C observed by the variable-temperature UV measurements agrees well with the DSC data and the changes observed in the Raman (Figure 7d) and X-ray diffractogram (Figure 4d) when the sample is heated to its high-temperature DSC transition.

When the sample was cooled to -40°C , no significant changes were observed in the UV spectrum and X-ray diffractogram (Figure 4a). This shows that no drastic structural changes are involved below the weak phase transition at -29°C .

The CPMAS/DD ^{29}Si NMR spectra of $(n\text{-Pr}_2\text{Si})_n$ at 25°C , showed only a single peak at -23.65 ppm ($\Delta\nu_{1/2} = 1.59\text{ ppm}$, 94.89 Hz). The CPMAS/DD ^{13}C NMR chemical shifts are reported in the Experimental Section.

B. Poly(diethylsilylene-co-di-*n*-propylsilylene). The first three members of the poly(di-*n*-alkylsilylene) series are shown to be crystalline with an *all-trans* conformation of the planar backbone and present no thermochromic effect below 170°C .²⁻⁵ In order to find out how a copolymer containing two members of this series might behave, we synthesized random poly(diethyl-co-di-*n*-propylsilylene), $(n\text{-Pr}_2\text{Si})_n(\text{Et}_2\text{Si})_m$. The copolymer composition was determined by integrating peaks in the ^1H and ^{29}Si NMR spectra in solution (Figure 8) and by pyrolysis-gas chromatography/mass spectroscopy (py-GC/MS) (Figure 9); the n/m values obtained were 0.83, 0.85, and 0.87 by these three independent methods.

The py-GC/MS experiments also provided information about the distribution of Et_2Si and $n\text{-Pr}_2\text{Si}$ groups along the copolymer chain (Figure 9 and Table 2). The pyrolysis-gas chromatogram at 300°C contains six peaks corresponding to the six possible cyclotetrasilanes composed of diethyl- and dipropylsilylene units. The assignment of the peaks was based on their mass spectra; the rationale for the assignment of peaks 3 and 4 is given elsewhere.²⁰ Summing up separately the molar amounts of the diethyl- and the dipropylsilylene units occurring in the different cyclotetrasilanes, the ratio of the sums gives the copolymer composition. The relative occurrence of the tetraethyl-, diethyldipropyl-, and tetrapropylidisilylene dyads in the

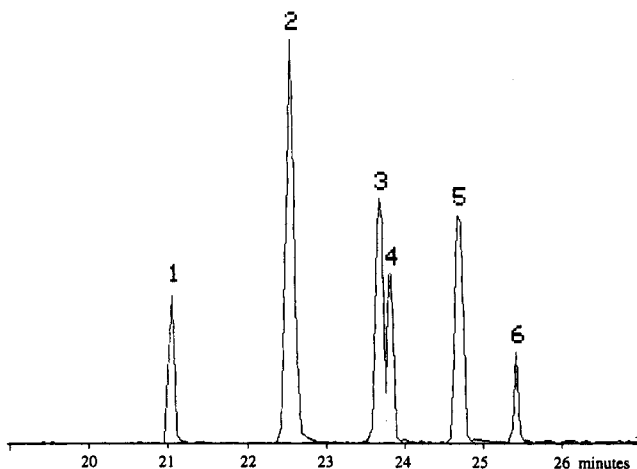


Figure 9. 300 °C pyrolysis-gas chromatogram showing four-membered rings from $(n\text{-Pr}_2\text{Si})_n(\text{Et}_2\text{Si})_m$: (1) Octaethyl-, (2) hexaethyldipropyl-, (3) 1,1,2,2-tetraethyl-3,3,4,4-tetrapropyl-, (4) 1,1,3,3-tetraethyl-2,2,4,4-tetrapropyl-, (5) diethylhexapropyl-, (6) octapropylcyclotetrasilane.

pyrolysate cyclotetrasilanes agrees very well with that calculated for a copolymer chain of random distribution with $n/m = 0.87$. The calculated percent values for the occurrence of dyads listed in Table 2 were obtained as described below:

dyads	calc relative occurrence
$[n\text{-Pr}_2\text{Si}]_2$	$\frac{0.87 \times 0.87 \times 100}{1.87} = 21.6\%$
$[n\text{-Pr}_2\text{Si}-\text{SiEt}_2]$	$2 \times \frac{0.87 \times 1.00 \times 100}{1.87} = 49.7\%$
$[\text{Et}_2\text{Si}]_2$	$\frac{1.00 \times 1.00 \times 100}{1.87} = 28.6\%$

The vibrational spectrum of the copolymer in the region 800–1600 cm^{-1} , where the bands of internal vibrations of alkyl substituents are situated, is just a sum of the spectra of the parent homopolymers, as can be clearly seen from Figure 10 where the three Raman spectra are compared. However in the region of the skeleton $\nu_{\text{Si}-\text{Si}}$ and $\nu_{\text{Si}-\text{C}}$ vibrations (300–750 cm^{-1}) the spectrum of the copolymer differs from the spectra of the parent homopolymers, as a consequence of the symmetry lowering due to the random distribution of the substituents along the backbone. For instance, there is no mutual exclusion for the $\nu_{\text{Si}-\text{Si}}$ vibrations, the Raman band at 434 cm^{-1} having an IR counterpart (Table 3). In addition, this Raman band is broad, but is not a superposition of the bands of the parent homopolymers.

The Raman pattern in the $\nu_{\text{Si}-\text{C}}$ region is rather simple, with only three lines, pointing to the absence of rotational isomerism about the Si–C bonds, *i.e.* to a significant order in the conformations of the side chains. It is interesting

to mention that the frequency of the intense $\nu_{\text{Si}-\text{C}}$ Raman line at 671 cm^{-1} nearly coincides with that in the spectrum of $(n\text{-Pr}_2\text{Si})_n$, indicating a similar conformation of the propyl substituent. However, the $\nu_{\text{Si}-\text{C}}$ vibration of the ethyl substituent at 615 cm^{-1} does not correspond in frequency to that of $(\text{Et}_2\text{Si})_n$, suggesting a different conformation for this group.

The powder X-ray diffraction pattern for $(n\text{-Pr}_2\text{Si})_n(\text{Et}_2\text{Si})_m$ (Figure 11a) shows that it is less crystalline than the respective homopolymers. The peaks corresponding to inter- and intramolecular d spacings were distinguished by analogy with the ones indexed for the homopolymers.^{4a} Those with 2θ values of 9.24, 13.41, and 20.98° were identified as 100, 110, and 210 peaks, having interchain components only. The corresponding d spacings of 9.55, 6.59, and 4.23 Å were consistent with a square lattice, where $a = b = 9.55$ Å. The peaks with an intrachain component, at 3.64 and 1.97 Å, were indexed as 101 and 002, respectively. At room temperature the copolymer exhibits a solid state UV band at 350 nm similar to both parent homopolymers (Figure 12). By analogy an *all-trans* planar structure, with a c -axis repeating unit of 3.94 Å, can be assigned to the copolymer backbone. Interestingly, when the X-ray diffractogram was obtained from a film cast from toluene, the pattern shows that the two peaks with intrachain components (101 and 002) are intensified in relation to all others (Figure 11b). This indicates that the polymer chains tend to crystallize oriented perpendicular to the glass slide, as the solvent slowly evaporates.

Variable-Temperature Studies of $(n\text{-Pr}_2\text{Si})_n(\text{Et}_2\text{Si})_m$. The DSC trace of the copolymer is shown in Figure 13. The copolymer exhibited a second-order transition at –18 °C and a first-order transition at 125 °C (onset at 113 °C) with $\Delta H = 4.14$ cal/g (17.3 J/g).

When $(n\text{-Pr}_2\text{Si})_n(\text{Et}_2\text{Si})_m$ was heated above the first-order DSC transition to 160 °C, the WAXD showed a single diffraction maximum at 9.70 Å (Figure 11c) in a pattern similar to the one for $(n\text{-Pr}_2\text{Si})_n$ and $(\text{Et}_2\text{Si})_n$ ^{3c} above their respective first-order DSC transitions and indicative of a mesomorphic phase with high interchain orientational order. The phase transition was also evident in the variable-temperature Raman spectra (Figure 14). Heating to about 100 °C caused no significant changes in the Raman spectrum, leading only to the usual overall decrease in intensity of the lines. On further heating, the relative intensity of the bands corresponding to the symmetrical skeletal vibrations in the region 200–700 cm^{-1} , decreased greatly; at about 120 °C the line at 236 cm^{-1} disappeared and the intensities of the symmetrical $\nu_{\text{Si}-\text{Si}}$ and $\nu_{\text{Si}-\text{C}}$ lines became comparable with those of their antisymmetric counterparts. Above the phase transition, the Raman spectrum is no longer enhanced by resonance.

The UV spectrum also changed dramatically when a film sample of the polymer was heated (Figure 12). At 80 °C the UV band at 350 nm acquired a shoulder at lower

Table 2. Quantitative Evaluation of the Pyrogram in Figure 9

peak no.	relative molar amount			relative occurrence		
	cyclic	Et_2Si	Pr_2Si	$\text{Et}_2\text{Si}-\text{SiEt}_2$	$\text{Pr}_2\text{Si}-\text{SiEt}_2$	$\text{Pr}_2\text{Si}-\text{SiPr}_2$
1	8.9	8.9		8.9		
2	28.0	21.0	7.0	14.0	14.0	
3	25.4	12.7	12.7	6.4	12.7	6.4
4	10.9	5.5	5.5		10.9	
5	21.4	5.4	16.0		10.7	10.7
6	5.4		5.4			5.4
total (%)	100.0	53.4	46.6	29.2	48.3	22.5
$n/m = 46.6/53.4 = 0.87$						
calcd % occurrence of dyads for random $(\text{Et}_2\text{Si})_n(\text{Pr}_2\text{Si})_m$ (see text)						
				28.6	49.7	21.6

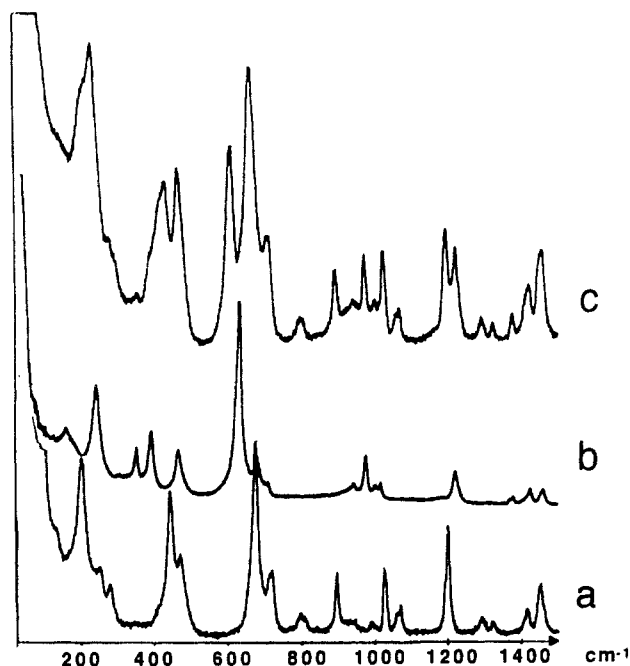


Figure 10. Raman spectra of (a) $(n\text{-Pr}_2\text{Si})_n$, (b) $(\text{Et}_2\text{Si})_n$, and (c) $(n\text{-Pr}_2\text{Si})_n(\text{Et}_2\text{Si})_m$ at 25 °C in the region 200–1600 cm^{-1} .

Table 3. IR and Raman Spectra of a Solid Sample of $(n\text{-Pr}_2\text{Si})_n(\text{Et}_2\text{Si})_m$ in the Region of the Skeleton Vibrations

Raman	IR	assgnt
357 (vw)	353 (m)	$\delta_{\text{Si}-\text{C}-\text{C}}$
434 (s br)	431 (m br)	$\nu_{\text{Si}-\text{Si}}$
472 (s)		$\nu_{\text{Si}-\text{Si}}$
	597 (m)	$\nu_{\text{Si}-\text{C}}$
615 (s)		$\nu_{\text{Si}-\text{C}}$
671 (vs)	666 (s)	$\nu_{\text{Si}-\text{C}}$
714 (m)		$\nu_{\text{Si}-\text{C}}$
	745 (m)	$\nu_{\text{Si}-\text{C}}$

wavelength, which grew as the temperature was increased. In the temperature interval 80–130 °C both bands coexisted, but at 140 °C the band at 350 nm disappeared completely, replaced by a very broad band at ca. 305 nm. These changes were reversible and indicate an equilibrium between two forms, the low-temperature *all-trans* conformation and a high-temperature mesomorphic phase, over this temperature range.

For the copolymer $(n\text{-Pr}_2\text{Si})_n(\text{Et}_2\text{Si})_m$, the CPMAS/DD ^{29}Si NMR spectrum at 25 °C shows two peaks: one at -24.94 ppm ($\Delta\nu_{1/2} = 2.70$ ppm, 161.06 Hz) from $^{29}\text{SiPr}_2$ units and another at -19.79 ppm ($\Delta\nu_{1/2} = 2.75$ ppm, 164.01 Hz) from $^{29}\text{SiEt}_2$ units. The $^{29}\text{SiPr}_2$ peak is shifted 1.29 ppm upfield and the $^{29}\text{SiEt}_2$ peak is shifted 1.41 ppm downfield from the peaks of their corresponding homopolymers ($[\text{Et}_2\text{Si}]_n$ ^{29}Si NMR, $\delta = -21.2$ ppm^{4a}). CPMAS/DD ^{13}C NMR chemical shifts are reported in the Experimental Section.

Conclusion

UV and Raman spectroscopy of $(n\text{-Pr}_2\text{Si})_n$ confirm the *all-trans* conformation of the silicon backbone,⁴ and show that the propyl side chains are present in only one conformation. A thermal transition was observed in the DSC and variable-temperature X-ray diffraction, UV, and Raman experiments. In correspondence with the behavior of the higher homologs,^{6–11} $(n\text{-Hex}_2\text{Si})_n$, $(n\text{-Pen}_2\text{Si})_n$, and $(n\text{-Bu}_2\text{Si})_n$, poly(di-*n*-propylsilylene) shows an UV absorption band around 315 nm above the high-temperature, first-order DSC transition. This suggests that a similar average conformation is present in the four above mentioned polymers in their disordered phases.

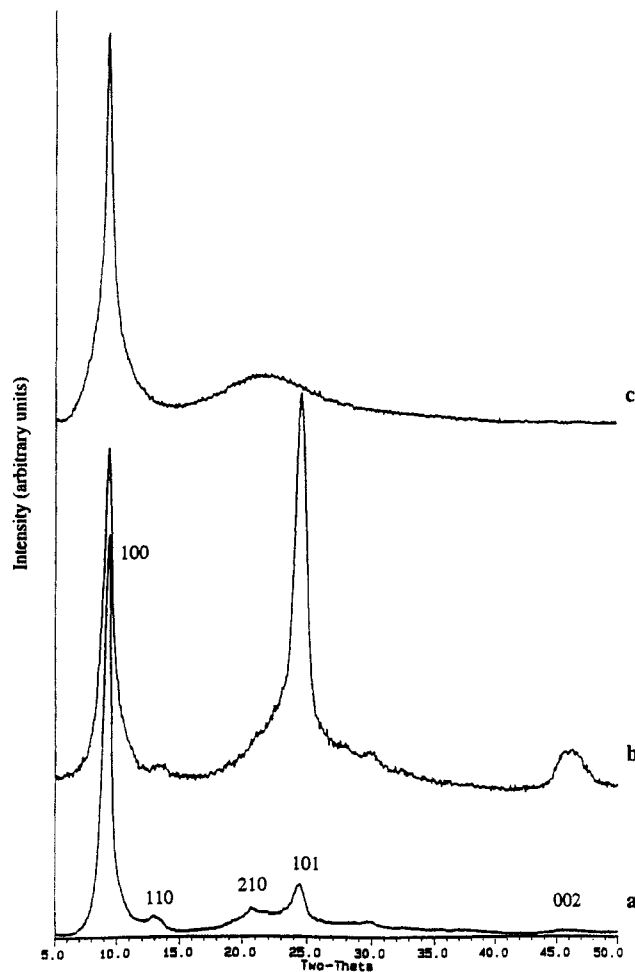


Figure 11. WAXD of $(n\text{-Pr}_2\text{Si})_n(\text{Et}_2\text{Si})_m$: (a) powder at 25 °C; (b) film at 25 °C; (c) powder at 160 °C.

In spite of its random nature, the copolymer $(n\text{-Pr}_2\text{Si})_n(\text{Et}_2\text{Si})_m$ is semicrystalline at room temperature, as indicated by X-ray diffraction, and has an *all-trans* conformation of the backbone, as indicated by UV spectroscopy. In the copolymer the crystal-mesophase transition temperature is 113 °C, about 100 deg lower than those for the corresponding homopolymers.

Experimental Section

Synthesis of Poly(di-*n*-propylsilylene). A 250 mL three-necked ambered-glass round bottom flask was equipped with a Friedrichs condenser connected to an argon inlet, a stirrer, and a pressure-equalized dropping funnel. Sodium metal (5.23 g, 0.23 mol) and 60 mL of dry toluene were introduced, and a sodium dispersion was prepared by stirring the mixture at reflux temperature for 15 min. $n\text{-Pr}_2\text{SiCl}_2$ (20 mL, 0.11 mol) was added from the dropping funnel in less than 1 min, and the mixture was allowed to react for 2 h under toluene reflux. The reaction mixture was allowed to cool to ambient temperature, quenched with 5 mL of a 2-propanol/sodium bicarbonate slurry, and then diluted with 800 mL of 2-propanol, and the polymer and salts were allowed to settle overnight. The polymer and insoluble salts were filtered out on a Büchner funnel, washed with water and dried at 60 °C in vacuum for 2 h. Purification was performed by refluxing the polymer in 150 mL of toluene for 5 h. Insoluble poly(di-*n*-propylsilylene) was filtered off the hot toluene solution and dried under vacuum (0.1 Torr) at 60 °C overnight (yield: 1.98 g, 15.6 %).

Synthesis of $(n\text{-Pr}_2\text{Si})_n(\text{Et}_2\text{Si})_m$. $n\text{-Pr}_2\text{SiCl}_2$ (10 mL, 0.055 mol) and Et_2SiCl_2 (8.2 mL, 0.055 mol) were added to a sodium dispersion (5.25 g, 0.238 mol) in 55 mL of refluxing toluene. Workup was similar to the one described for $(n\text{-Pr}_2\text{Si})_n$, except for the purification procedure which was done by dissolving the copolymer in hot toluene and reprecipitating it with 2-propanol.

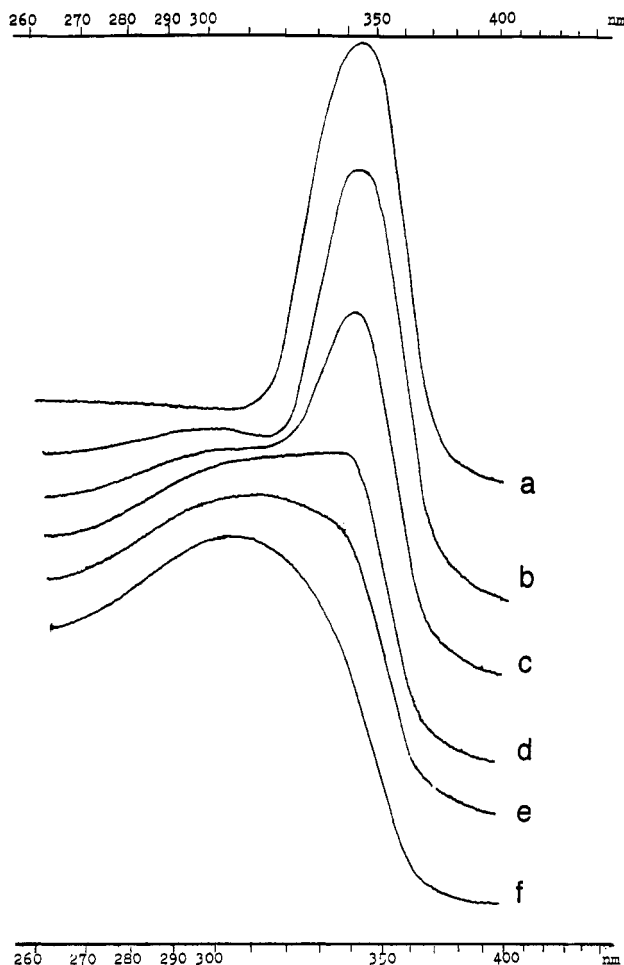


Figure 12. Variable-temperature UV spectra of solid $(n\text{-Pr}_2\text{Si})_n(\text{Et}_2\text{Si})_m$: (a) 25 °C, (b) 80 °C, (c) 110 °C, (d) 120 °C, (e) 130 °C, (f) 140 °C.

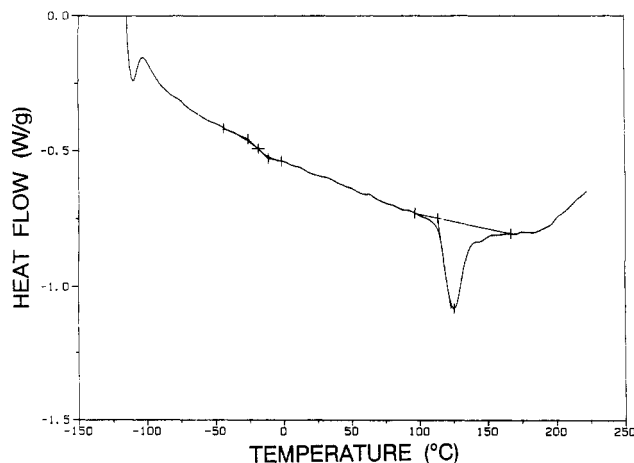


Figure 13. DSC of $(n\text{-Pr}_2\text{Si})_n(\text{Et}_2\text{Si})_m$ obtained at a heating rate of 10 °C/min, after cooling the sample from +230 to -120 °C at 320 °C/min.

Yield of $(n\text{-Pr}_2\text{Si})_n(\text{Et}_2\text{Si})_m$: 2.17 g (21%). $M_w = 14\,000$. PD = 2.2. ^1H NMR: δ - 1.74 ($\text{SiCH}_2\text{CH}_2\text{CH}_3$, peak area = 2.0), 1.34 ($\text{SiCH}_2\text{CH}_2\text{CH}_3$, SiCH_2CH_3), 1.30 (SiCH_2CH_3), 1.19 ppm ($\text{SiCH}_2\text{CH}_2\text{CH}_3$, triplet, $^3J_{\text{H-H}} = 6.5$ Hz, peak area = 3.0). ^{29}Si NMR: δ = -23.4 ($^{29}\text{SiPr}_2$), -19.1 ppm ($^{29}\text{SiEt}_2$). The peaks at 1.34, 1.40, and 1.19 ppm have a total area of 11.03. The n/m ratio was obtained by subtracting the five protons of the propyl group from 11.03. The total area from the ethyl protons was then equal to 6.02 and from the n -propyl protons equal to 7. For $n/m = 1$ the propyl to ethyl integration ratio is 7/5; therefore $\text{Pr}/\text{Et} = 7.0/6.03$ gives us $n/m = 0.83$.

$n\text{-Pr}_2\text{SiCl}_2$ and Et_2SiCl_2 were purchased from Hüls America, Inc. and distilled over potassium carbonate under N_2 prior to

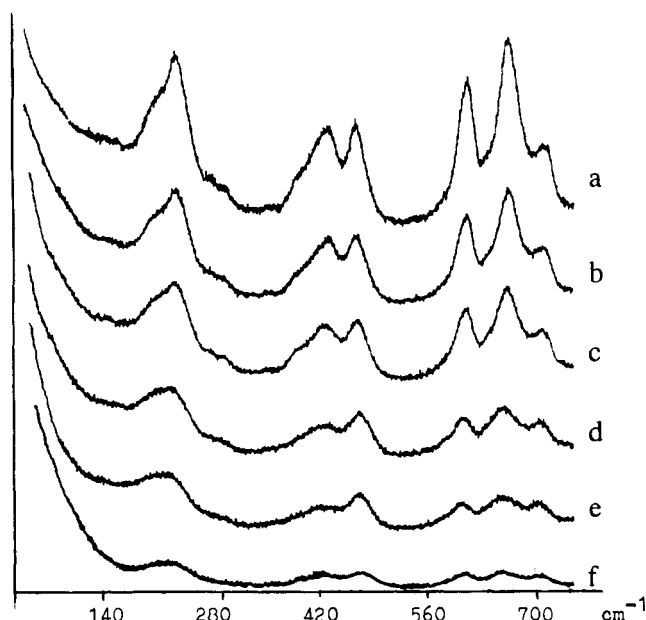


Figure 14. Variable-temperature Raman spectra of $(n\text{-Pr}_2\text{Si})_n(\text{Et}_2\text{Si})_m$: (a) 25 °C, (b) 60 °C, (c) 80 °C, (d) 100 °C, (e) 125 °C and (f) 140 °C.

use. Toluene was distilled from benzophenone ketyl under N_2 and transferred to the reaction flask with a syringe. Sodium metal was cut fresh under mineral oil, washed quickly with dry hexane, and added to the reaction flask. A positive flow of argon was maintained at all times during polymerization.

Molecular weights were measured by gel permeation chromatography using a Waters Associates Model 6000A liquid chromatograph equipped with three American Polymer Standards Corp. Ultrastaygel columns in series with porosity indices of 10^3 , 10^4 , and 10^5 Å and THF as eluant. The polymers were detected with a Waters Model 440 ultraviolet absorbance detector at a wavelength of 254 nm, and the data were manipulated using a Waters Model 745 data module. Molecular weights were determined relative to a calibration from polystyrene standards.

^1H (500 MHz) and ^{29}Si (100.33 MHz) NMR spectra in solution were measured on a Bruker AM-500 with 10% (w/w) solutions of polymers in benzene- d_6 using Me_4Si as reference.

Films for X-ray diffraction of $(n\text{-Pr}_2\text{Si})_n(\text{Et}_2\text{Si})_m$ were cast from a toluene slurry and dried in a vacuum oven for 12 h at 60 °C. Measurements of powder and film polymer samples were done on a Nicolet I2/V diffractometer, with a $\text{Cu K}\alpha$ beam.

DSC measurements were performed with a 2910 TA Instruments and a 2200 TA Instruments controller using mass samples of 10–11 mg in a dry helium atmosphere. Calibration was performed with mercury and indium.

Thermogravimetric analyses were performed with a 2950 TA Instruments and a 2100 TA Instruments controller under N_2 flow with a heating rate of 10 °C/min, using 8–10 mg of sample. Thermogravimetric analysis of the copolymer $(n\text{-Pr}_2\text{Si})_n(\text{Et}_2\text{Si})_m$ showed a gradual weight loss of 1.17% up to 222 °C, probably a result of moisture or solvent contamination. A smooth decomposition step from 222 to 329 °C resulted in a mass loss of 15%. A second abrupt decomposition step was observed at 329 °C with a total mass loss of 44%. This stepwise decomposition pattern is common in a number of di-*n*-alkylsilylene copolymers²¹ and the onset of the first step at 222 °C is in the range reported for the decomposition onset of other di-*n*-alkylpolysilanes (e.g. $(\text{Me}_2\text{Si})_n$ at 250 °C, $(\text{Pen}_2\text{Si})_n$ at 220 °C, and $(\text{Hex}_2\text{Si})_n$ at 226 °C).¹⁶

Cross-polarized microscopy was done under N_2 flow in a Karl Zeiss microscope equipped with a heating stage, using a magnification of 800.

The Raman spectra were obtained on samples sealed in glass capillaries, using a Ramanor HG-2S and U-1000 laser Raman spectrometers, excited by the 5145-Å line of an ILA-2 Ar⁺ laser. The IR spectra were examined using an M-80 Karl Zeiss spectrophotometer and a Bruker IFS-113 Fourier transform spectrometer. The samples were either KBr or CsI pellets or

Nujol mulls. The UV spectra of solid polymers pressed between quartz plates were determined with an M-40 Karl Zeiss spectrophotometer. The temperature dependence of Raman and UV spectra was studied using a specially designed high-temperature cell with an electrical heating device.

Pyrolysis was performed in a Pyroprobe 120 (Chemical Data System, Oxford, PA) equipped with a platinum coil and quartz sample tube interfaced either to a Hewlett-Packard 5985 B gas chromatograph/mass spectrometer or to a Hewlett-Packard 5880A gas chromatograph with flame ionization detector. The sample mass was about 100 μg . A helium carrier gas at a flow rate of 20 mL/min purged the pyrolysis chamber which was held at 250 °C. The flow was split in a ratio of 1/20 before being introduced into the gas chromatograph. The GC separation was performed on a temperature-programmed fused silica capillary column (20 m \times 0.2 mm) coated with SE-52 or OV-1 phase. The gas chromatography was coupled to the mass spectrometer through a deactivated fused-silica capillary tube introduced into the ion source, and kept at 300 °C. The mass spectrometer was operated in the electron-impact mode at 70 eV. The area values of the peaks in Figure 9 detected by a flame ionization detector were transformed to the relative molar amounts reported in Table 2.

The magic angle spinning cross-polarized dipolar decoupled (CPMAS/DD) 75.429 MHz ^{13}C and 59.591 MHz ^{29}Si NMR spectra were recorded on a Varian Unity 300 spectrometer using an 8 mm Doty Scientific Inc. magic angle spinning probe and sapphire rotors. Contact time = 3000 s, relaxation delay = 2 s, number of scans = 100, spinning rate = 3000 Hz, high-power proton dipolar decoupling level = 50 kHz.

Chemical shifts (ppm) for solid state ^{29}Si NMR (referenced to TMS): for $(n\text{-Pr}_2\text{Si})_n$ (−23.65); for $(n\text{-Pr}_2\text{Si})_n(\text{Et}_2\text{Si})_m$ $^{29}\text{SiPr}_2$ (−24.95), $^{29}\text{SiEt}_2$ (−19.80). Chemical Shifts (ppm) for solid state ^{13}C NMR (referenced to hexamethylbenzene at 132 ppm): for $(n\text{-Pr}_2\text{Si})_n$ Si—CH₂—CH₂—CH₃ (17.60); Si—CH₂—CH₂—CH₃ (21.29), Si—CH₂—CH₂—CH₃ (20.12); for $(n\text{-Pr}_2\text{Si})_n(\text{Et}_2\text{Si})_m$ Si—CH₂—CH₂—CH₃ (19.54), Si—CH₂—CH₂—CH₃ (22.26), Si—CH₂—CH₂—CH₃ (23.43), Si—CH₂—CH₃ (8.46), Si—CH₂—CH₃ (13.13).

Acknowledgment. This research partly supported by a grant from the U.S. Office of Naval Research. The pyrolysis-GC/MS work was supported by the Hungarian National Research Fund (OTKA), under Contract No. 3078. The work of the Russian authors was supported by a grant from the Russian Fund for Fundamental Investigations (Grant No. 93-02-16242) and also from the International Science Foundation (Grant No. MED 000).

References and Notes

- (1) For reviews see: Miller, R. D.; Michl, J. *Chem. Rev.* **1989**, *89*, 1353. West, R. In *The Chemistry of Organosilicon Compounds*; Patai, S.; Rappaport, Z., Eds.; John Wiley & Science: New York, 1989; pp 1207–1240. Zeigler, J. *Synth. Met.* **1989**, *28*, C581.
- (2) (a) Lovinger, A. J.; Davis, D. D.; Schilling, F. C.; Padden, F. J., Jr.; Bovey, F. A.; Zeigler, J. M. *Macromolecules* **1991**, *24*, 132. (b) Furukawa, S.; Takeuchi, K. *Solid State Commun.* **1993**, *87* (10), 931.
- (3) (a) Leites, L. A.; Dement'ev, V. V.; Bukalov, S. S.; Yadritseva, T. S.; et al. *Izv. Akad. Nauk SSSR, Ser. Khim.* **1989**, 2869 (*Proceedings of the Academy of Sciences of the USSR, Chemical Series*). (b) Leites, L. A.; Bukalov, S. S.; Yadritseva, T. D.; Mochov, M. K.; Autipova, B. A.; Frunze, T. M.; Dement'ev, V. V. *Macromolecules* **1992**, *25*, 2991.
- (4) (a) Lovinger, A. J.; Davis, D. D.; Schilling, F. C.; Bovey, F. A.; Zeigler, J. M. *Polym. Commun.* **1989**, *30*, 356. (b) Furukawa, S.; Takeuchi, K.; Mizoguchi, M.; Shimana, M.; Tamura, M. *J. Phys.: Condens. Matter* **1993**, *5*, L461.
- (5) Leites, L. A.; Bukalov, S. S.; Yadritseva, T. D.; Autipova, B. A.; Frunze, T. M.; Dement'ev, V. V. *Polym. Sci.* **1992**, *34A*, 980.
- (6) Walsh, C. A.; Schilling, F. C.; Macgregor, R. A., Jr.; Lovinger, A. J.; Davis, D. D.; Bovey, F. A.; Zeigler, J. M. *Synth. Met.* **1989**, *28*, C599.
- (7) Schilling, F. C.; Lovinger, A. J.; Zeigler, J. M.; Davis, D. D.; Bovey, F. A. *Macromolecules* **1989**, *22*, 3055.
- (8) Miller, R. D.; Farmer, B. L.; Fleming, W. W.; Sooriyakumaran, R.; Rabolt, J. F. *J. Am. Chem. Soc.* **1987**, *109*, 2509.
- (9) (a) Lovinger, A. J.; Schilling, F. C.; Bovey, F. A.; Zeigler, J. M. *Macromolecules* **1986**, *19*, 2657. (b) Schilling, F. C.; Bovey, F. A.; Lovinger, A. J.; Zeigler, J. M. *Macromolecules* **1986**, *19*, 2657. (c) McCrary, V. R.; Sette, F.; Chen, C. T.; Lovinger, A. J.; Robin, M. B.; Stoehr, J.; Zeigler, J. M. *J. Chem. Phys.* **1988**, *88*, 5925. (d) Hallmark, V. M.; Sooriyakumaran, R.; Miller, R. D.; Rabolt, J. F. *J. Chem. Phys.* **1989**, *90*, 2486.
- (10) Rabolt, J. F.; Hofer, D.; Miller, R. D.; Fickes, F. N. *Macromolecules* **1986**, *19*, 611.
- (11) Kuzmany, H.; Rabolt, J. F.; Farmer, B. L.; Miller, R. D. *J. Chem. Phys.* **1986**, *85*, 7413.
- (12) Symmetrical polysilanes with still larger alkyl chains adopt a *trans-gauche-trans-gauche'* structure. See: Karikari, G. K.; Gresco, A. J.; Farmer, B. L.; Miller, R. D.; Rabolt, J. F. *Macromolecules* **1993**, *26*, 3937.
- (13) Cutler, D. J.; Hendra, P. J.; Fraser, G. In *Laser Raman Spectroscopy on Synthetic Polymers*; Painter, P. C., Coleman, M. M., König, J. L., Eds.; Theory of Vibrational Spectroscopy and its Applications to Polymer Materials; John Wiley & Sons: New York, 1982; p 71.
- (14) Hassler, K. *Spectrochim. Acta* **1984**, *40a*, 775.
- (15) Ernst, C. A.; Allred, A. L.; Ratner, M. A. *J. Organomet. Chem.* **1979**, *178*, 119.
- (16) Varma-Nair, M.; Cheng, J.; Jin, Y.; Wunderlich, B. *Macromolecules* **1991**, *24*, 5442.
- (17) Weber, P.; Guillon, D.; Skoulios, A.; Miller, R. D. *Liq. Cryst.* **1990**, *8* (6), 825.
- (18) Bukalov, S. S.; Leites, L. A. To be published.
- (19) Bukalov, S. S.; Leites, L. A. *Izv. Akad. Nauk. SSSR, Ser. Fiz.*, **1989**, *53*, 1715. (*Proceedings of the Academy of Sciences of the USSR Physical Series*).
- (20) Blazsó, M. *Rapid Comm. Mass Spectrom.* **1991**, *5*, 507.
- (21) Menescal, R.; West, R. Unpublished results.